**Smart Structures and Systems**, *Vol. 15, No. 6 (2015) 1503-1520*
DOI: http://dx.doi.org/10.12989/sss.2015.15.6.1503 

# A novel solution for thick-walled cylinders made of functionally graded materials

Y.Z. Chen*

*Division of Engineering Mechanics, Jiangsu University, Zhenjiang, Jiangsu, 212013, P.R. China*

*(Received September 5, 2013, Revised April 1, 2014, Accepted April 10, 2014)*

**Abstract.** This paper provides a novel solution for thick-walled cylinders made of functionally graded materials (FGMs). In the formulation, the cylinder is divided into N layers. On the individual layer, the Young's modulus is assumed to be a constant. For an individual layer, two undetermined constants are involved in the elastic solution. Those undetermined coefficients can be evaluated from the continuation condition along interfaces of layers and the boundary conditions at the inner surface and outer surface of cylinder. Finally, the solution for thick-walled cylinders made of functionally graded materials is obtainable. This paper provides several numerical examples which are useful for engineer to design a cylinder made of FGMs.

**Keywords:** functionally graded materials; thick-walled cylinder; numerical technique; multiply-layered cylinder

## 1. Introduction

Since the thick-walled cylinders made of functionally graded materials are widely used in engineering structures, the problem for finding the stress state for the thick-walled cylinders made of functionally graded materials (FGMs) was studied by many researchers (Zhang and Hasebe 1996, Jabbari *et al.* 2002, Shi *et al.* 2007, Tutuncu 2007, Theotokoglou and Stampouloglou 2008, Li and Peng 2009, Horgan and Chan 1999, Chen and Lin 2010, Arefi *et al*. 2012).

In an earlier year, an exact elasticity solution was developed for a radially nonhomogeneous hollow circular cylinder of exponential Young's modulus and constant Poisson ' s ratio (Zhang and Hasebe 1996). A general analysis of one-dimensional steady-state thermal stresses in a hollow thick cylinder made of functionally graded material was developed (Jabbari *et al*. 2002). Two different kinds of heterogeneous elastic hollow cylinders were studied (Shi *et al*. 2007). One is a cylinder with multi-layers and another is a cylinder with continuously graded properties. Stress analysis for a thick-walled FGM cylinders with exponentially-varying properties was studied, and a governing equation for radial displacement was suggested. A series form solution for the displacement was suggested (Tutuncu 2007). The plane axisymmetric problem with axisymmetric geometry and loading was analyzed for a radially nonhomogeneous circular cylinder (Theotokoglou and Stampouloglou 2008). Exact solutions for radial deformations of a functionally

*Corresponding author, Dr., E-mail: chens@ujs.edu.cn

**Copyright © 2015 Techno-Press, Ltd.**
http://www.techno-press.org/?journal=sss&subpage=8 ISSN: 1738-1584 (Print), 1738-1991 (Online)

graded isotropic and incompressible second-order elastic cylinder were found (Batra and Iaccarino 2008).

For the mentioned problem, the associated elastic problem in the functionally graded cylinder was reduced to a Fredholm integral equation (Li and Peng 2009). By approximately solving the resulting equation, the distribution of the radial and circumferential stresses can be determined. Recently, numerical techniques were developed to solve the mentioned problem (Horgan and Chan 1999, Chen and Lin 2010). The plane strain static deformations of a functionally graded hollow cylinder under both axisymmetric and non-axisymmetric loads were studied (Nie and Batra 2010). Both the Young's modulus and the Poisson's ratio are assumed in the form of power law variation. The problem is solved by using the Airy stress function. Analytical solutions for thick-walled cylinders made of functionally graded materials were obtained (Sburlati 2012). In the study, two kinds of Young's modulus variation, or the power law and the exponential law, along the radius of cylinder were suggested. The obtained numerical results and solutions are helpful for materials scientists to design the FGM cylinders.

We see from above-mentioned references that, if the Young's modulus is an arbitrary function in the radial direction, some difficulties for the problem remain. For example, many researchers assumed that the Young's modulus had a power function or an exponential function.

In this paper, the Young's modulus in radial direction is assumed to be an arbitrary function, and the Poisson's ratio takes a constant value. The cylinder is divided into N layers. Along the individual layer, we assume the Young's modulus is a constant. Alternatively speaking, the Young's modulus in radial direction is approximated by a step function. For an individual layer, two undetermined constants are involved in the elastic solution. Those undetermined coefficients can be evaluated from the continuation condition along interfaces of layers and the boundary conditions at the inner surface and outer surface of cylinder. After evaluating those coefficients, the displacement and the stress state in the cylinler is determined accordingly. Several numerical examples are presented in the paper. The obtained result shows that the FGMs property has a significant influence to the stress distribution. Numerical results are given which are useful for engineer to design a cylinder made of FGMs.

## 2. Analysis

In a problem for the thick-walled cylinder, the displacement in the r-direction is denoted by "u". Two strain components can be expressed as (Chen and Lin 2010, Timoshenko and Goodier 1970)

$$\varepsilon_r = \frac{du}{dr}, \qquad \varepsilon_\theta = \frac{u}{r} \tag{1}$$

In the present study, the Young's modulus E(r) is an arbitrary function, and the Poisson's ratio takes a constant value $\nu = 0.3$. In the plane strain case, the stress-strain relation takes the form

$$\varepsilon_r = \frac{1-\nu^2}{E(r)}\left(\sigma_r - \frac{\nu}{1-\nu}\sigma_\theta\right) \tag{2}$$

$$\varepsilon_\theta = \frac{1-\nu^2}{E(r)}\left(\sigma_\theta - \frac{\nu}{1-\nu}\sigma_r\right) \tag{3}$$

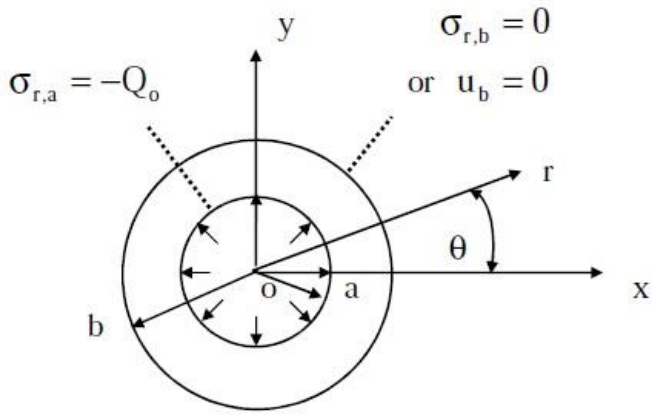


Fig. 1 Boundary value problem for thick-walled cylinders made of functionally graded materials

From Eqs. (2) and (3), we can express the stresses $\sigma_r$ and $\sigma_r$ through the strains $\varepsilon_r$ and $\varepsilon_\theta$. Further, after using Eq. (1), the stress components can be expressed as

$$\sigma_r = \frac{E(r)(1-\nu)}{(1+\nu)(1-2\nu)}\left(\frac{du}{dr}+\frac{\nu}{1-\nu}\frac{u}{r}\right) \tag{4}$$

$$\sigma_\theta = \frac{E(r)(1-\nu)}{(1+\nu)(1-2\nu)}\left(\frac{u}{r}+\frac{\nu}{1-\nu}\frac{du}{dr}\right) \tag{5}$$

The detailed expression for the Young's modulus E(r) will be defined in the concrete example. Clearly, from the symmetric condition of deformation, the shear stress $\sigma_{r\theta}$ and the shear strain $\varepsilon_{r\theta}$ are generally vanishing.

In the symmetrical deformation case, the equilibrium equation for the stress components $\sigma_r$ and $\sigma_\theta$ takes the form (Timoshenko and Goodier 1970)

$$\frac{d\sigma_r}{dr}+\frac{\sigma_r-\sigma_\theta}{r}=0 \tag{6}$$

Substituting Eqs. (4) and (5) into Eq. (6) yields

$$\frac{d^2u}{dr^2}+\frac{1}{r}\frac{du}{dr}-\frac{u}{r^2}+\left(\frac{du}{dr}+\frac{\nu}{1-\nu}\frac{u}{r}\right)\frac{1}{E(r)}\frac{dE(r)}{dr}=0 \tag{7}$$

The cylinder is assumed within the range $a \le |r| \le b$ (Fig. 1). In the formulation, the boundary condition is as follows

$$\sigma_r \big|_{r=a} = \sigma_{r,a} = -Q_o, \qquad \sigma_r \big|_{r=b} = \sigma_{r,b} = 0 \tag{8}$$

where $Q_o$ is a given loading.

Without losing the generality, we first consider the problem for functionally cylinder with the following elastic property

$$E(r) = E_o\{1+\beta\sin(\frac{\pi(r-a)}{2(b-a)})\} \tag{9}$$

where $\beta$ and $E_o$ are two elastic constants. Thus, the Young's modulus has the following properties

$$E(r) \big|_{r=a} = E_o, \qquad E(r) \big|_{r=b} = E_o(1+\beta) \tag{10}$$

The Poisson's ratio takes a constant value $\nu = 0.3$ in the present paper.

In the formulation, we assume that the cylinder is composed of many layers and the elastic constants take constant value in the individual layer (Fig. 2). The cylinder is divided into N layers. The radii are denoted by $r = r_1$ ($r_1 = a$), $r = r_2$, … $r = r_j$, $r = r_{j+1}$,… and $r = r_{N+1}$ ($r_{N+1} = b$), respectively.

Clearly, at $r = r_j$, and $r = r_{j+1}$ we have $E(r) \big|_{r=r_j} = E_o\{1+\beta\sin(\frac{(j-1)\pi}{2N})\}$ and $E(r) \big|_{r=r_{j+1}} = E_o\{1+\beta\sin(\frac{j\pi}{2N})\}$, respectively. Therefore, for the j-th layer defined by $r_j \le r \le r_{j+1}$, the relevant Young's modulus is approximated by a constant value

$$E_j = E_o\{1+\beta\sin(\frac{(j-0.5)\pi}{2N})\} \approx E_o\{(1+\beta\sin(\frac{(j-1)\pi}{2N})) + (1+\beta\sin(\frac{j\pi}{2N}))\}/2, \quad (r_j \le r \le r_{j+1}) \tag{11}$$

That is to say, for j=1,2,…N, the $E_j$ value changes from $E_j = E_o\{1+\beta\sin[0.5\pi/(2N)]\}$ (j=1), $E_j = E_o\{1+\beta\sin[1.5\pi/(2N)]\}$ (j=2), …. to $E_j = E_o\{1+\beta\sin[(N-0.5)\pi/(2N)]\}$ (j=N).

Since Young's elastic modulus (or $E_j$) is constant for the j-th layer defined along $r_j \le r \le r_{j+1}$, Eq. (7) becomes

$$\frac{d^2u}{dr^2} + \frac{1}{r}\frac{du}{dr} - \frac{u}{r^2} = 0, \qquad (r_j \le r \le r_{j+1}) \tag{12}$$

Clearly, from Eq. (12), we have a general solution (Timoshenko and Goodier 1970)

$$u_j(r) = g_j f_1(r) + h_j f_2(r), (r_j \le r \le r_{j+1}) \tag{13}$$

where $g_j$ and $h_j$ (j=1,2,…N) denote some undetermined coefficients and

$$f_1(r) = r \ , \qquad f_2(r) = \frac{1}{r} \tag{14}$$

Substituting the obtained function "u" into Eqs. (4) and (5), two stress component $\sigma_r$ and $\sigma_\theta$ are obtainable

$$\sigma_{r,j}(j) = g_j f_{3,j}(r) + h_j f_{4,j}(r) \qquad (r_j \le r \le r_{j+1}) \tag{15}$$

$$\sigma_{\theta,j}(j) = g_j f_{5,j}(r) + h_j f_{6,j}(r) \qquad (r_j \le r \le r_{j+1}) \tag{16}$$

where

$$f_{3,j}(r) = \frac{E_j}{(1+\nu)(1-2\nu)}, \qquad f_{4,j}(r) = -\frac{E_j}{(1+\nu)r^2} \tag{17}$$

$$f_{5,j}(r) = \frac{E_j}{(1+\nu)(1-2\nu)}, \qquad f_{6,j}(r) = \frac{E_j}{(1+\nu)r^2} \tag{18}$$

In Eqs. (17) and (18), $E_j$ denotes a constant Young's modulus of elasticity which is defined on the j-th layer ($r_j \le r \le r_{j+1}$).

The task in the study is to evaluate the $g_j$ and $h_j$ (j=1,2,…N) values from the continuation condition along the interfaces of layers and the boundary conditions.

Along the interface of the j-th layer ($r_j \le r \le r_{j+1}$) and j+1-th layer ($r_{j+1} \le r \le r_{j+2}$), we have the following continuation condition for displacement

$$u_j \big|_{r=r_{j+1}} = u_{j+1} \big|_{r=r_{j+1}}, \qquad (j=1,2,\ldots N\text{-}1) \tag{19}$$

From Eq. (13), Eq. (19) can be rewritten as

$$g_j f_1(r_{j+1}) + h_j f_2(r_{j+1}) = g_{j+1} f_1(r_{j+1}) + h_{j+1} f_2(r_{j+1}), \quad (j=1,2,\ldots N\text{-}1) \tag{20}$$

Similarly, the continuation condition for the stress is as follows

$$\sigma_{r,j} \big|_{r=r_{j+1}} = \sigma_{r,j+1} \big|_{r=r_{j+1}}, \qquad (j=1,2,\ldots N\text{-}1) \tag{21}$$

From Eq. (15), Eq. (21) can be rewritten as

$$g_j f_{3,j}(r_{j+1}) + h_j f_{4,j}(r_{j+1}) = g_{j+1} f_{3,j+1}(r_{j+1}) + h_{j+1} f_{4,j+1}(r_{j+1}), \ (j=1,2,\ldots N\text{-}1) \tag{22}$$

From traction condition along the inner surface shown by Eq. (8), or from Eq. (15), we have

$$\sigma_{r,1} \big|_{r=r_1} = g_1 f_{3,1}(r_1) + h_1 f_{4,1}(r_1) = -Q_o \tag{23}$$

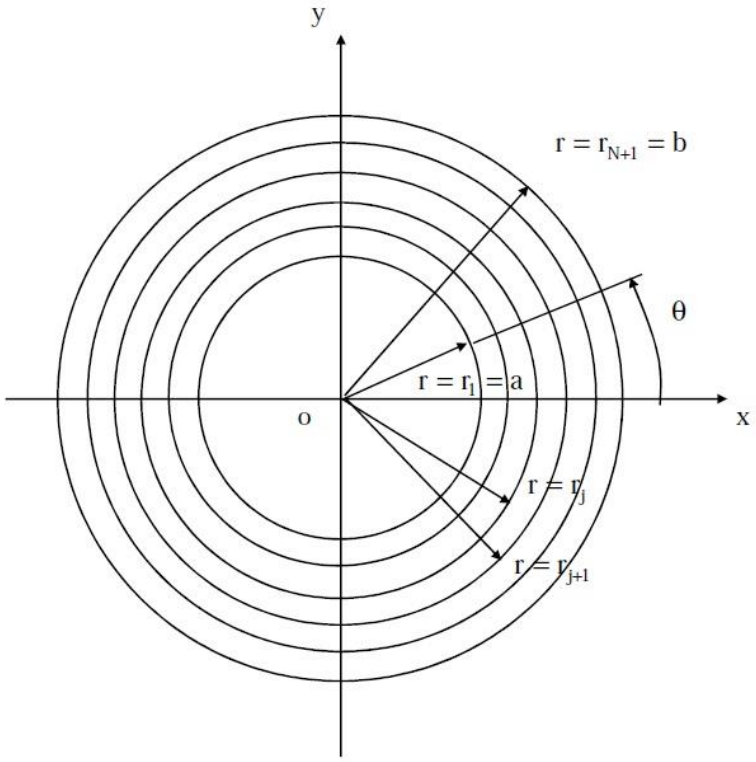


Fig. 2 A cylinder composed of N layers

Similarly, from traction free condition along the outer surface shown by Eq. (8), or from Eq. (15), we have

$$\sigma_{r,N}\big|_{r=r_{N+1}} = g_N f_{3,N}(r_{N+1}) + h_N f_{4,N}(r_{N+1}) = 0 \tag{24}$$

From Eqs. (20),(22),(23) and (24), we have total 2N equations for $g_j$ and $h_j$ (j=1,2,…N). Thus, those coefficients $g_j$ and $h_j$ (j=1,2,…N) can be determined exactly. Further, the displacement and stresses in all layers can be evaluated by using Eqs. (13) to (18).

In order to express the numerical solution more clearly, we choose the case N=3 for an example. In this case, we have six unknowns $g_j$ and $h_j$ (j=1,2,3) in Eqs. (20),(22),(23),(24), and $r_1 = a$, $r_2 = (2a+b)/3$, $r_3 = (a+2b)/3$, $r_4 = b$. In addition, from Eqs. (20),(22),(23) and (24), we can formulate the following algebraic equation

$$[\mathbf{M}]\{X\} = \{Y\} \tag{25}$$

where

$$[\mathbf{M}]=\begin{vmatrix} f_1(r_2) & f_2(r_2) & -f_1(r_2) & -f_2(r_2) & 0 & 0 \\ f_{3,1}(r_2) & f_{4,1}(r_2) & -f_{3,2}(r_2) & -f_{4,2}(r_2) & 0 & 0 \\ 0 & 0 & f_1(r_3) & f_2(r_3) & -f_1(r_3) & -f_2(r_3) \\ 0 & 0 & f_{3,2}(r_3) & f_{4,2}(r_3) & -f_{3,3}(r_3) & -f_{4,3}(r_3) \\ f_{3,1}(r_1) & f_{4,1}(r_1) & 0 & 0 & 0 & 0 \\ 0 & 0 & 0 & 0 & f_{3,3}(r_4) & f_{4,3}(r_4) \end{vmatrix} \tag{26}$$

$$\{X\}=(g_1 \quad h_1 \quad g_2 \quad h_2 \quad g_3 \quad h_3)^T \tag{27}$$

$$\{y\}=(0 \quad 0 \quad 0 \quad 0 \quad -Q_o \quad 0)^T \tag{28}$$

Note that, the first four columns in the matrix $[\mathbf{M}]$ are derived from Eqs. (20) and (22). The fifth column in the matrix $[\mathbf{M}]$ is derived from Eq. (23). In addition, the sixth column in the matrix $[\mathbf{M}]$ is derived from Eq. (24), Therefore, we can obtain the solution for $g_j$ and $h_j$ (j=1,2,3) from Eq. (25). For the arbitrary value of "N", we can get the solution for $g_j$ and $h_j$ (j=1,2,…N) in a similar manner.

## 3. Numerical examples

Three numerical examples are introduced below. Several forms of elastic property E(r) are assumed in examples. The influences for displacement and stresses from the assumed E(r) distribution are studied in details.

Example 1

In the first example (Fig. 3(a)), the Young's modulus is assumed to be

$$E(r)=E_o\{1+\beta\sin(\frac{\pi(r-a)}{2(b-a)})\} \tag{29}$$

Thus, we have $E(a)/E_o=1$, and $E(b)/E_o=1+\beta$ (Fig. 3(a)).

For the j-th layer ($r_j \le r \le r_{j+1}$), the relevant Young's modulus is approximated by

$$E(r)=E_o\{1+\beta\sin(\frac{(j-0.5)\pi}{2N})\} \qquad (\text{along } r_j \le r \le r_{j+1},\ j=1,2..N) \tag{30}$$

In the computation, N=100 and a/b=0.5 are adopted. The boundary condition for the cylinder is as follows

$$\sigma_r\big|_{r=r_1}=\sigma_r\big|_{r=a}=-Q_o \tag{31}$$

$$\sigma_r\big|_{r=r_{N+1}}=\sigma_r\big|_{r=b}=0 \tag{32}$$

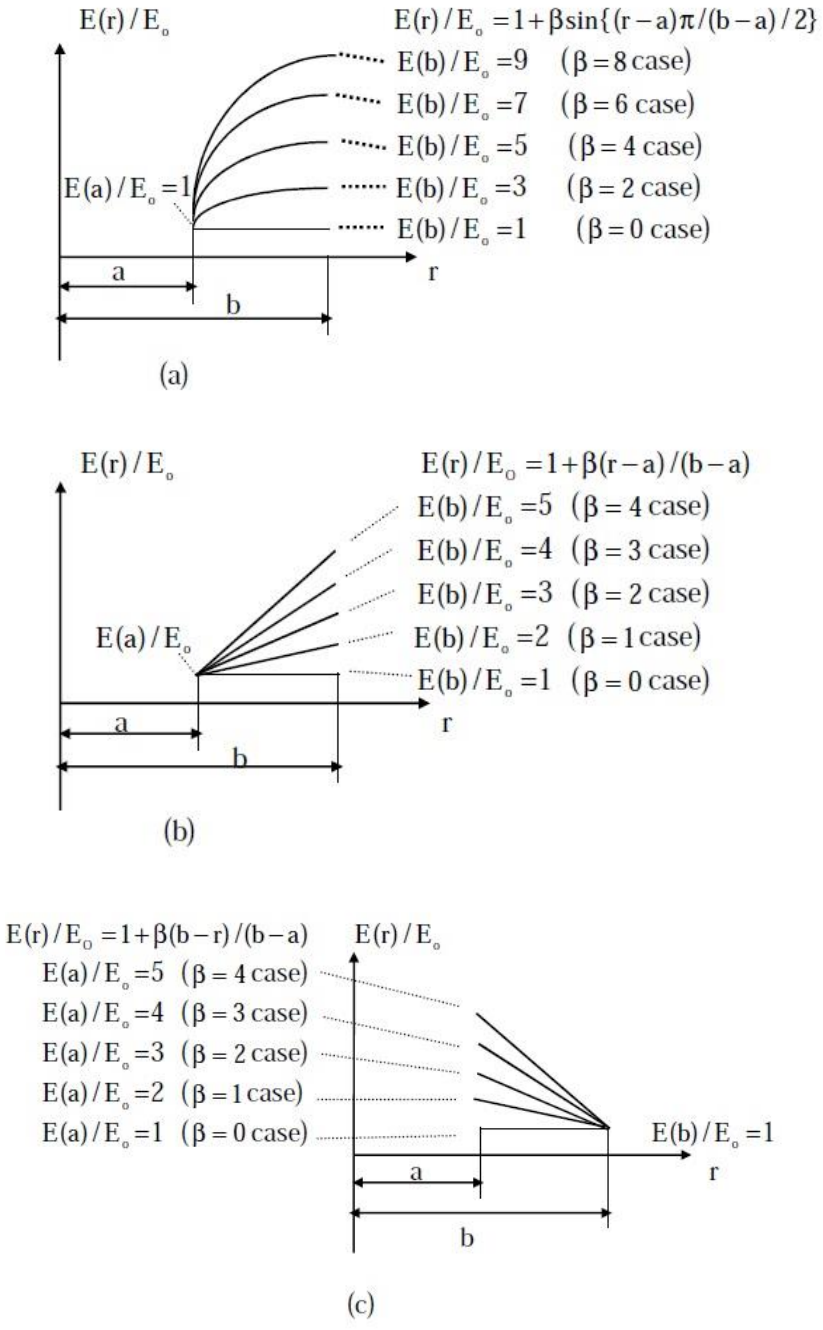


Fig. 3 (a) functionally graded cylinder with the elastic property $E(r)/E_o = 1+\beta\sin\{(r-a)\pi/(b-a)/2\}$, (b) functionally graded cylinder with the elastic property $E(r)/E_O = 1+\beta(r-a)/(b-a)$, (c) functionally graded cylinder with the elastic property $E(r)/E_O = 1+\beta(b-r)/(b-a)$

As claimed previously, from Eqs. (20),(22),(23) and (24), we can evaluate the coefficients $g_j$ and $h_j$ (j=1,2,…N) exactly. Therefore, the displacement and stresses in N layers can be evaluated exactly. Therefore, the displacement and stress components in the range $a \le r \le b$ can be finally determined.

The computed results for displacement and stresses are expressed as

$$u = S(\beta,(r-a)/(b-a))\frac{bQ_o}{E_o}, \qquad (a \le r \le b, \text{ or } 0 \le (r-a)/(b-a) \le 1) \tag{33}$$

$$\sigma_r = T_r(\beta,(r-a)/(b-a))Q_o, \qquad (a \le r \le b, \text{ or } 0 \le (r-a)/(b-a) \le 1) \tag{34}$$

$$\sigma_\theta = T_\theta(\beta,(r-a)/(b-a))Q_o, \qquad (a \le r \le b, \text{ or } 0 \le (r-a)/(b-a) \le 1) \tag{35}$$

The calculated results for S, $T_r$ and $T_\theta$ under the conditions: (a) $a/b = 0.5$ and (b) $\beta =$ 0,2,4,6 and 8 , five cases, are plotted in Figs. 4-6, respectively.

From the plotted results, we see that the material parameter $\beta$ can significantly affect the displacement and stress distribution. For example, at the point r=a, we have S=0.949, 0.496, 0.341, 0.262 and 0.213 ( S- non-dimensional displacement for u ) for $\beta$ =0,2,4,6 and 8, respectively ( Fig. 4). In fact, there is a lowest résistance for deformation for the case $\beta$ =0. Thus, the S curve for the case $\beta$ =0 is located in the upper position in Fig. 4.

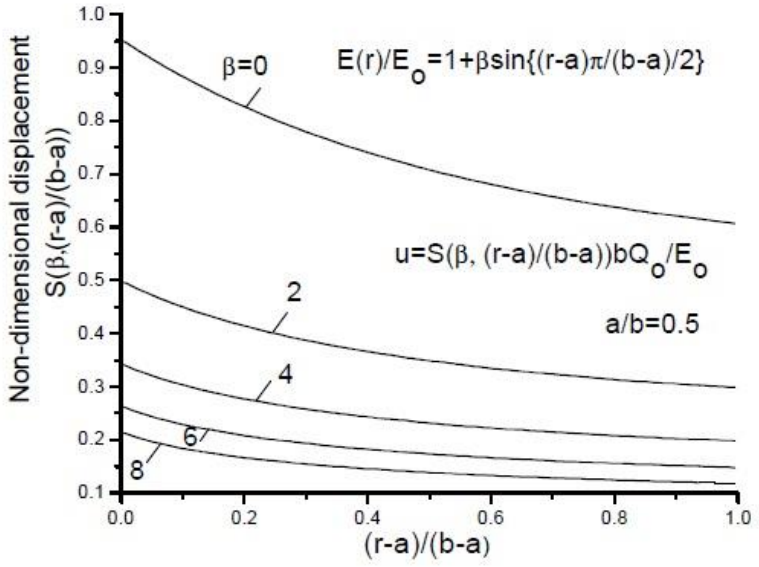


Fig. 4 Non-dimensional displacement $S(\beta,(r-a)/(b-a))$ for the displacement "u " with the elastic property $E(r) = E_o\{1+\beta\sin[(r-a)\pi/(b-a)/2]\}$ ( see Fig. 3(a) and Eq. (33))

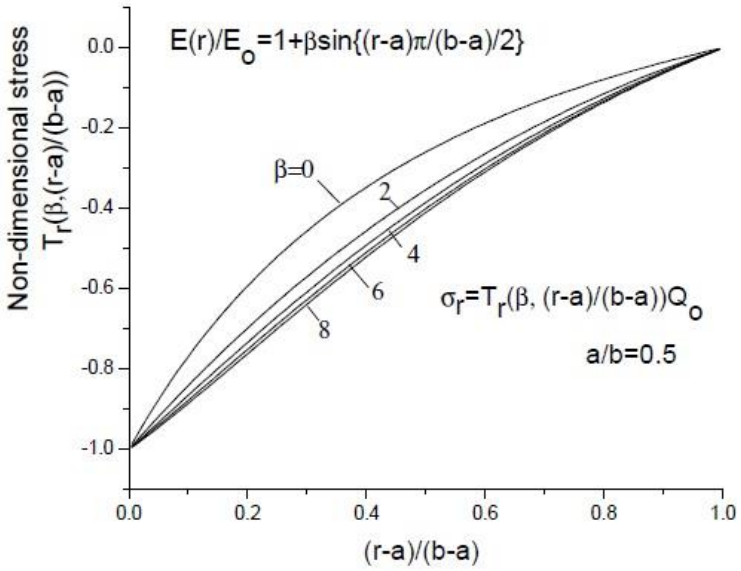


Fig. 5 Non-dimensional stress $T_r(\beta,(r-a)/(b-a))$ for the stress $\sigma_r$ with the elastic property $E(r)=E_o\{1+\beta\sin[(r-a)\pi/(b-a)/2]\}$ ( see Fig. 3(a) and Eq. (34))

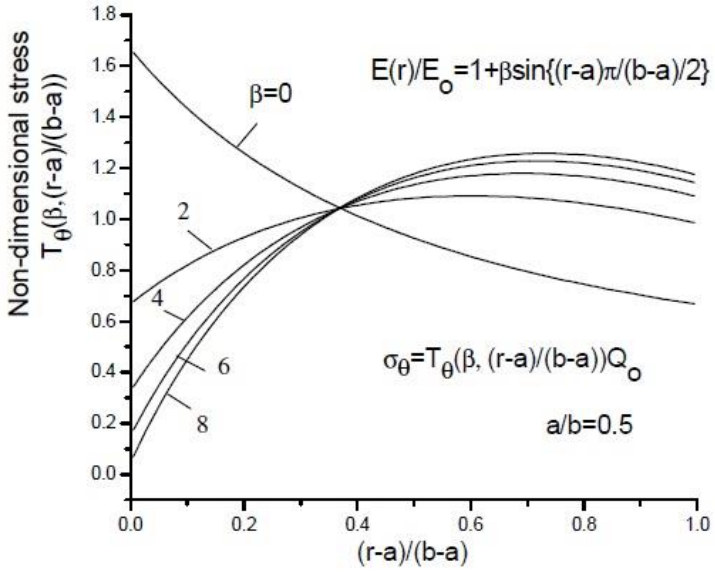


Fig. 6 Non-dimensional stress $T_\theta(\beta,(r-a)/(b-a))$ for the stress $\sigma_\theta$ with the elastic property

$E(r) = E_o\{1+\beta\sin[(r-a)\pi/(b-a)/2]\}$ ( see Fig. 3(a) and Eq. (35))

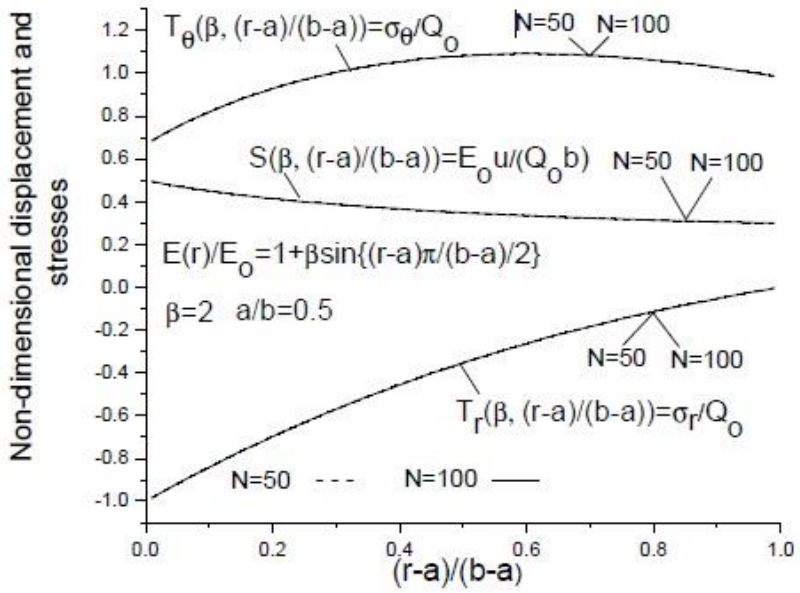


Fig. 7 Comparison results for (1) non-dimensional displacement $S(\beta,(r-a)/(b-a))$ ,(2) non-dimensional stress $T_r(\beta,(r-a)/(b-a))$ and (3) non-dimensional stress $T_\theta(\beta,(r-a)/(b-a))$ under different N ( N=50 and N=100)

For the $\sigma_r$ component, it changes from $T_r=-1$( r=a) to $T_r=0$ (r=b), gradually (Fig. 5).

For the $\sigma_\theta$ component in the case of $\beta=0$, it changes from $T_\theta=1.653$ ( r=a) to $T_\theta=0.668$ (r=b)( Fig. 6). For the $\sigma_\theta$ component in the case of $\beta=8$, it changes from $T_\theta=0.069$ ( r=a) to $T_\theta=1.176$ (r=b). Clearly, in the case of $\beta=8$, we have $E(r)\big|_{r=a}=E_o$ and $E(r)\big|_{r=b}=9E_o$. That is to say, the outer circle surface of cylinder is more rigid, and it is subject to a higher stress.

In order to examine the accuracy achieved in the present paper, under the conditions (a) a/b=0.5, (b) $\beta=2$, we perform a computation for two cases of N=50 and N=100 (N- number of the assumed layers). The computed results for non-dimensional displacement and stresses, or $S(\beta,(r-a)/(b-a))=\dfrac{E_o u}{Q_o b}$, $T_r(\beta,(r-a)/(b-a))=\dfrac{\sigma_r}{Q_o}$ and $T_\theta(\beta,(r-a)/(b-a))=\dfrac{\sigma_\theta}{Q_o}$, are plotted in Fig. 7. From Fig. 7 we see that, the computed curves for N=50 and N=100 are merged into the same curve. This figure proves that a higher accuracy and a convergent tendency have been achieved in the presented method.

Example 2

In the second example (Fig. 3(b)), the Young's modulus is assumed to be

$$E(r) = E_o(1+\beta(r-a)/(b-a)) \tag{36}$$

Thus, we have $E(a)/E_o = 1$, and $E(b)/E_o = 1+\beta$ ( Fig. 3(b)).

For the j-th layer ( $r_j \le r \le r_{j+1}$ ), the relevant Young's modulus is approximated by

$$E_j = E_o(1+\beta(j-0.5)/N) \qquad (\text{along } r_j \le r \le r_{j+1},\ j=1,2..N) \tag{37}$$

In the computation, N=100 and a/b=0.5 are adopted. The boundary condition for the cylinder is as follows

$$\sigma_r \big|_{r=r_1} = \sigma_r \big|_{r=a} = -Q_o \tag{38}$$

$$\sigma_r \big|_{r=r_{N+1}} = \sigma_r \big|_{r=b} = 0 \tag{39}$$

The numerical procedure is same as for the first example.

The computed results for displacement and stresses are expressed as

$$u = S(\beta,(r-a)/(b-a))\frac{bQ_o}{E_o}, \qquad (a \le r \le b, \text{ or } 0 \le (r-a)/(b-a) \le 1) \tag{40}$$

$$\sigma_r = T_r(\beta,(r-a)/(b-a))Q_o, \qquad (a \le r \le b, \text{ or } 0 \le (r-a)/(b-a) \le 1) \tag{41}$$

$$\sigma_\theta = T_\theta(\beta,(r-a)/(b-a))Q_o, \qquad (a \le r \le b, \text{ or } 0 \le (r-a)/(b-a) \le 1) \tag{42}$$

The calculated results for S, $T_r$ and $T_\theta$ under the conditions: (a) $a/b = 0.5$ and (b) $\beta =$ 0,1,2,3 and 4, five cases, are plotted in Figs. 8-10, respectively.

From the plotted results, we see that the material parameter $\beta$ can significantly affect the displacement and stress distribution. For example, at the point r=a, we have S=0.949, 0.705, 0.560, 0.472 and 0.407 (S- non-dimensional displacement for u ) for $\beta$ =0,1,2,3 and 4, respectively (Fig. 8). In fact, there is a lowest résistance for deformation for the case $\beta$ =0. Thus, the S curve for the case $\beta$ =0 is located in the upper position in Fig. 8.

For the $\sigma_r$ component, it changes from $T_r = -1$( r=a) to $T_r$ =0 (r=b), gradually (Fig. 9).

For the $\sigma_\theta$ component in the case of $\beta = 0$ (homogenous case), it changes from $T_\theta = 1.653$ ( r=a) to $T_\theta = 0.668$ (r=b) (Fig. 10). Clearly, $T_\theta$ in the case of $\beta = 0$ is a descending one. For the $\sigma_\theta$ component in the case of $\beta = 4$, it changes from $T_\theta = 0.482$ ( r=a) to $T_\theta = 1.296$ (r=b). That is to say, the outer rigid surface ( r=b) is subject to a higher stress.

Example 3

In the third example (Fig. 3(c)), the Young's modulus is assumed to be

$$E(r) = E_o(1+\beta(b-r)/(b-a)) \tag{43}$$

Thus, we have $E(a)/E_o = 1+\beta$ and $E(b)/E_o = 1$ (Fig. 3(c )).

For the j-th layer ( $r_j \le r \le r_{j+1}$ ), the relevant Young's modulus is approximated by

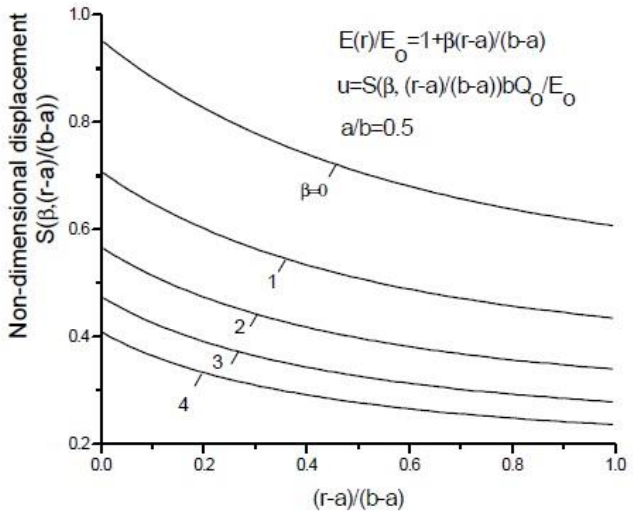


Fig. 8 Non-dimensional displacement $S(\beta,(r-a)/(b-a))$ for the displacement "u " with the elastic property $E(r)=E_o(1+(\beta(r-a)/(b-a))$ ( see Fig. 3(b) and Eq. (40))

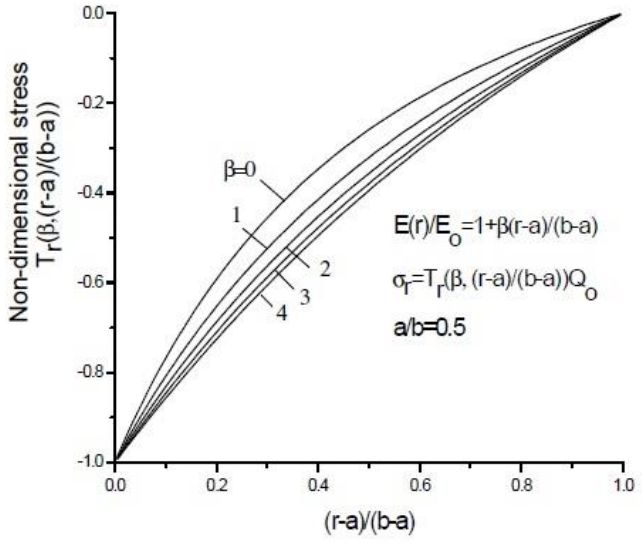


Fig. 9 Non-dimensional stress $T_r(\beta,(r-a)/(b-a))$ for the stress $\sigma_r$ with the elastic property $E(r)=E_o(1+(\beta(r-a)/(b-a))$ ( see Fig. 3(b) and Eq. (41)

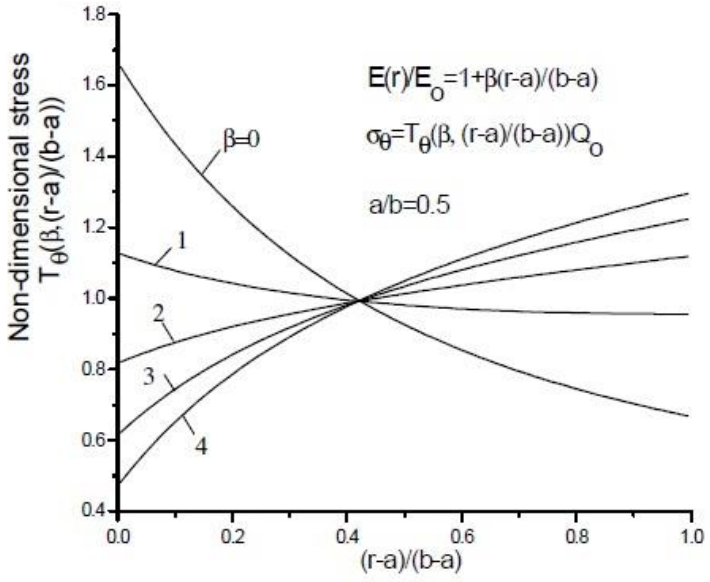


Fig. 10 Non-dimensional stress $T_\theta(\beta,(r-a)/(b-a))$ for the stress $\sigma_\theta$ with the elastic property $E(r)=E_o(1+(\beta(r-a)/(b-a))$ ( see Fig. 3(b) and Eq. (42)

$$E_j = E_o(1+\beta(N-j+0.5)/N) \qquad \text{(along } r_j \le r \le r_{j+1},\ j=1,2..N) \tag{44}$$

In the computation, N=100 and a/b=0.5 are adopted. The boundary condition for the cylinder is as follows

$$\sigma_r\big|_{r=r_1} = \sigma_r\big|_{r=a} = -Q_o \tag{45}$$

$$\sigma_r\big|_{r=r_{N+1}} = \sigma_r\big|_{r=b} = 0 \tag{46}$$

The numerical procedure is same as for the first example.

The computed results for displacement and stresses are expressed as

$$u = S(\beta,(r-a)/(b-a))\frac{bQ_o}{E_o}, \qquad (a \le r \le b, \text{ or } 0 \le (r-a)/(b-a) \le 1) \tag{47}$$

$$\sigma_r = T_r(\beta,(r-a)/(b-a))Q_o, \qquad (a \le r \le b, \text{ or } 0 \le (r-a)/(b-a) \le 1) \tag{48}$$

$$\sigma_\theta = T_\theta(\beta,(r-a)/(b-a))Q_o, \qquad (a \le r \le b, \text{ or } 0 \le (r-a)/(b-a) \le 1) \tag{49}$$

The calculated results for S, $T_r$ and $T_\theta$ under the conditions: (a) $a/b=0.5$ and (b) $\beta=$

0,1,2,3 and 4, five cases, are plotted in Figs. 11-13, respectively.

From the plotted results, we see that the material parameter $\beta$ can significantly affect the displacement and stress distribution. For example, at the point r=a, we have S=0.949, 0.578, 0.417, 0.326 and 0.257 ( S- non-dimensional displacement for u ) for $\beta$ =0,1,2,3 and 4, respectively (Fig. 11). In fact, there is a lowest résistance for deformation for the case $\beta$ =0. Thus, the S curve for the case $\beta$ =0 is located in the upper position in Fig. 11.

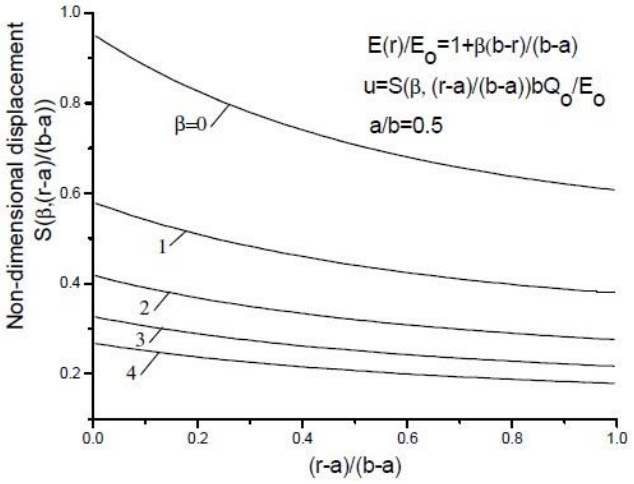


Fig. 11 Non-dimensional displacement $S(\beta,(r-a)/(b-a))$ for the displacement "u " with the elastic property $E(r)=E_o(1+(\beta(b-r)/(b-a))$ ( see Fig. 3(c) and Eq. (47))

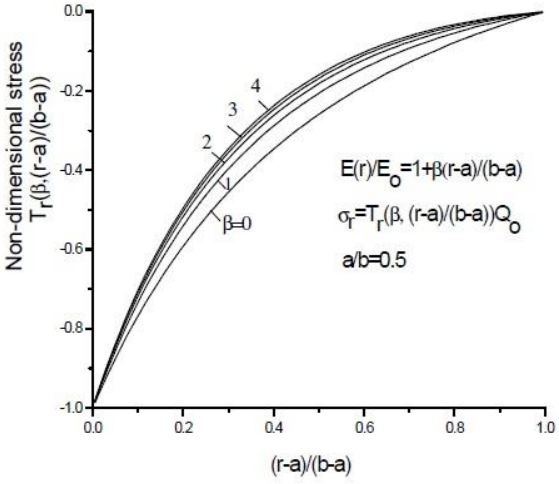


Fig. 12 Non-dimensional stress $T_r(\beta,(r-a)/(b-a))$ for the stress $\sigma_r$ with the elastic property $E(r)=E_o(1+(\beta(b-r)/(b-a))$ (see Fig. 3(c) and Eq. (48))

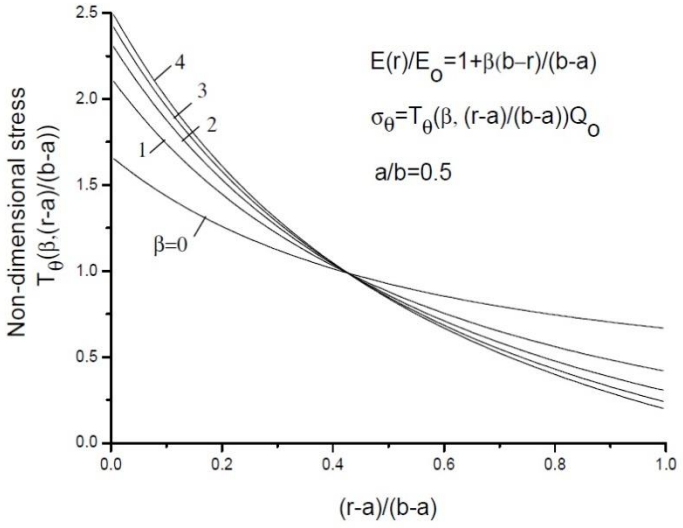


Fig. 13 Non-dimensional stress $T_\theta(\beta,(r-a)/(b-a))$ for the stress $\sigma_\theta$ with the elastic property $E(r)=E_o(1+(\beta(b-r)/(b-a))$ ( see Fig. 3(c) and Eq. (49)).

For the $\sigma_r$ component, it changes from $T_r=-1$( r=a) to $T_r=0$ (r=b), gradually (Fig. 12).

For the $\sigma_\theta$ component in the case of $\beta=0$ (homogenous case), it changes from $T_\theta=1.653$ ( r=a) to $T_\theta=0.668$ (r=b) (Fig. 13). For the $\sigma_\theta$ component in the case of $\beta=4$, it changes from $T_\theta=2.490$ ( r=a) to $T_\theta=0.201$ (r=b). In this case, both $T_\theta$ curves ($\beta=0$ and $\beta=4$) are descending. From Fig.13, we see that the inner rigid surface ( r=a) is subject to a higher stress for $\sigma_\theta$.

Example 4

In the fourth example, except for the Young's modules all the conditions are same as in the three previous examples. In the example, the Young's modulus is assumed as

$$E(r)=E_o\exp\{\beta(r-a)/(b-a)\} \tag{50}$$

Thus, we have $E(a)/E_o=1$ and $E(b)/E_o=\exp\beta$. The boundary condition is still expressed as $\sigma_r\big|_{r=a}=-Q_o$ and $\sigma_r\big|_{r=b}=0$. The same technique used in the previous examples is used to solve the problem.

The non-dimensional stresses are still expressed in the form of Eqs. (48) and (49). In the conditions of (1) a/b=0.5 and (2) $\beta=$ -2, -1, 0 1,2, the computed results for non-dimensional stresses $T_r(\beta,(r-a)/(b-a))=\dfrac{\sigma_r}{Q_o}$ and $T_\theta(\beta,(r-a)/(b-a))=\dfrac{\sigma_\theta}{Q_o}$ are plotted in Figs. (14)

and (15) with solid line, respectively. In addition, the previously obtained results are also plotted in those figures with dash line. From Figs. (14) and (15) we see that two sets of curves are merged in to the same curve. Therefore, the accuracy of the present method is proved.

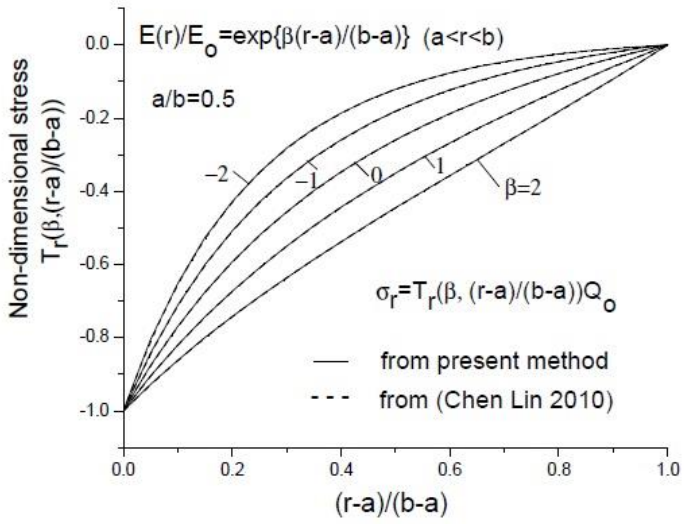


Fig. 14 Comparison results for non-dimensional stress $T_r(\beta,(r-a)/(b-a))$ with the elastic property $E(r)=\exp\{\beta(r-a)/(b-a)\}$.

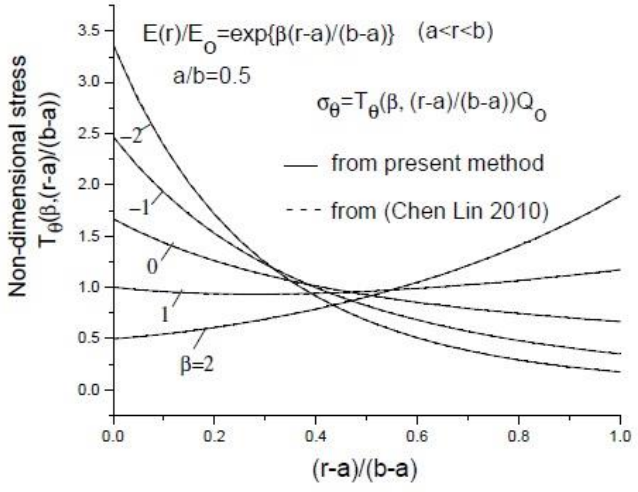


Fig. 15 Comparison results for non-dimensional stress $T_\theta(\beta,(r-a)/(b-a))$ with the elastic property $E(r)=\exp\{\beta(r-a)/(b-a)\}$

## 4. Conclusions

This paper provides a universal solution for thick-walled cylinders made of functionally graded materials with arbitrary Young's modulus of elasticity in the radial direction. It is an important step to approximate the Young's modulus of elasticity by a step function. The cylinder is divided into N layers. Since the Young's modulus of elasticity is constant on the individual layer, the usual solution of cylinder for homogenous materials can be used to the individual layer. Several numerical examples are carried out in the present study. It is proved that the property of the functionally graded materials has significant influence to the stress state of the FGMs cylinder.

## References

Arefi, M., Rahimi, G.H. and Khoshgoftar, M.J. (2012), "Exact solution of a thick walled functionally graded piezoelectric cylinder under mechanical, thermal and electrical loads in the magnetic field", *Smart Struct. Syst.*, **9**(5), 427-439.

Batra, R.C. and Iaccarino, G.L. (2008), "Exact solutions for radial deformations of a functionally graded isotropic and incompressible second-order elastic cylinder", *Int. J. Nonlinear Mech.*, **43**(5), 383-398.

Chen, Y.Z. and Lin, X.Y. (2010), "An alternative numerical solution of thick-walled cylinders and spheres made of functionally graded materials", *Comput. Mater. Sci.*, **48**(3), 640-647.

Horgan, C.O. and Chan, A.M. (1999), "The stress response of functionally graded isotropic linearly elastic rotating disks", *J. Elasticity*, **55**(3), 219-230.

Jabbari, M., Sohrabpour, S. and Eslami, M.R. (2002), "Mechanical and thermal stresses in a functionally graded hollow cylinder due to radially symmetric loads", *Int. J. Pres. Vessels and Pip.*, **79**(7), 493-497.

Li, X.F. and Peng, X.L. (2009), "A pressurized functionally graded hollow cylinder with arbitrarily varying material properties", *J. Elasticity*, **96**(1), 81-95.

Nie, G.J. and Batra, R.C. (2010), "Exact solutions and material tailoring for functionally graded hollow circular cylinders", *J. Elasticity*, **99**(2), 179-201.

Sburlati, R. (2012), "Analytical elastic solutions for pressurized hollow cylinders with internal functionally graded coatings", *Comput. Struct.*, **94**(12), 3592-3600.

Shi, Z.F., Zhang, T.T. and Xiang, H.J. (2007), "Exact solutions of heterogeneous elastic hollow cylinders", *Comput. Struct.*, **79**, 140-147.

Theotokoglou, E.E. and Stampouloglou, I.H. (2008), "The radially nonhomogeneous elastic axisymmentric problem", *Int. J. Solids Struct.*, **45**, 6535-6552.

Timoshenko, S.P. and Goodier, J.N. (1970), *Theory of Elasticity*, McGraw-Hill Book Company, New York.

Tutuncu, N. (2007), "Stresses in thick-walled FGM cylinders with exponentially-varying properties", *Eng. Struct.*, **29**(9), 2032-2035.

Zhang, X.Z. and Hasebe, N. (1996), "Elasticity solution for a radically nonhomogeneous hollow circular cylinder", *J. Appl. Mech. - ASME*, **66**(3), 599-606.

*CC*